Journal of Materials Chemistry B

ROYAL SOCIETY OF CHEMISTRY

PAPER

View Article Online
View Journal | View Issue

Cite this: *J. Mater. Chem. B*, 2021, **9**, 7167

Molecule-specific vibration-based chiral differentiation of Raman spectra using cysteine modified gold nanoparticles: the cases of tyrosine and phenylalanine

Xueping Sun,† Ning Wang,† Yanxiu He, Huanjun Kong, Haifeng Yang* and Xinling Liu *

Received 1st May 2021,
Accepted 30th June 2021

DOI: 10.1039/d1tb00983d

rsc.li/materials-b

The chirality of amino acids plays a key role in many biochemical processes, with the development of spectroscopic analysis methods for the chiral differentiation of amino acids being significant. Normal Raman spectroscopy is blind to chirality; however, chiral discrimination of tyrosine (Tyr) (or phenylalanine, Phe) enantiomers using Raman spectra can be achieved assisted by the construction of a simple chiral selector (*i.e.*, cysteine (Cys)-modified Au nanoparticles (NPs)). Due to the synergetic effect between Cys and the Au NPs, the characteristic Raman scattering intensities of the Tyr (or Phe) enantiomer with the same chirality of Cys are enantioselectively boosted by over four-fold compared with those of the counter enantiomer of Tyr (or Phe). The large differences in the Raman signals allow for the determination of enantiomeric excess. Interestingly, such enantiomeric discrimination is not revealed by the common chiral analysis method of circular dichroism spectroscopy. Consequently, it is anticipated that Raman spectroscopy based on molecular vibrations will find broad applications in chirality-related detection with high sensitivity and species specificity.

Introduction

A pair of chiral molecules with a mirror-image relationship in their configurations are known as enantiomers, which are indistinguishable in many ways, such as their chemical compositions. However, their chemical, biological and pharmacological activities may be different, for example, with one enantiomer of a chiral drug displaying therapeutic effects and the other showing unexpected side effects.[1] Therefore, the development of analytical methods for the enantioselective recognition and assessment of enantiomeric excess (e.e.) are of great importance.[2] Amino acids exist in D- and L-configurations. In our bodies, however, L-amino acids are preferably employed as the basic building blocks of proteins, which remains a great mystery of life.[3] As for D-amino acids, their appearance in living organisms may be associated with many diseases.[4] As a result, amino acids are significant models in chiral differentiation, and understanding the enantioselectivity of amino acids *in vitro* will shed light on the intermolecular interactions related to chiral selection mechanisms *in vivo* and the biochemical/pharmaceutical applications of artificial nanomaterials.[5–8]

College of Chemistry and Materials Science, Shanghai Normal University, Shanghai 200234, China. E-mail: hfyang@shnu.edu.cn, xlliu@shnu.edu.cn
† The authors contribute equally to this work.

Chiral discrimination can be achieved *via* either "matter-matter" or "matter-light" chiral interactions. Typically, chromatographic techniques are efficient in separating enantiomers based on their enantioselective interactions with chiral stationary phases, mobile phases or additives.[9] Nevertheless, these methods require expensive columns, time-consuming operations and professional skills. Electronic circular dichroism (CD) spectroscopy is another common chiral analysis route that uses chiral light (*i.e.*, circularly polarized light, CPL) as the selector, which is fulfilled by measuring the difference in the absorption of the left- and right-handed CPL of chiral molecules.[10] In principle, CD signals are a result of the electronic transitions of chromophores and/or auxochromes in chiral environments. However, the absorption wavelengths of these transitions of organic molecules are overlapped in the ultraviolet region, which makes it difficult for molecule-specific identification to some degree. Moreover, the CD signals of many biomolecules are intrinsically weak and thus incapable of detection in some situations. Consequently, alternative strategies are indispensable in overcoming the aforementioned limitations of chromatographic and CD methods.[9,11]

Raman spectroscopy can provide valuable information about molecular structures and intra-/inter-molecular interactions through the fingerprint information of molecular vibrations, and is a well-accepted analysis tool with significant advantages in terms of specificity, sensitivity and speed.[12] Nevertheless, unlike

CD spectroscopy, normal Raman instruments are unable to directly distinguish a pair of enantiomers due to the absence of CPL-related optic units. On the other hand, chiral discrimination in intermolecular interactions has been proven to be feasible. Hence, the collection and analysis of optical signals representing these chiral interactions will contribute towards chirality detection. For example, nuclear magnetic resonance (NMR) spectroscopy is also blind to chirality because a pair of enantiomers give the same chemical shifts; however, a chiral auxiliary can be employed to interact with enantiomers and transform them into diastereomers that have different electronic surroundings, which are then distinguishable in NMR spectra.[13] Gold (Au) nanostructures with surface enhanced Raman scattering (SERS) effects are always used as substrates for Raman detection. Furthermore, the modification of Au nanostructures allows for various physical and/or chemical interactions for chirality detection.[14–17] In a recent example,[18] vertically-aligned gold nanorods were modified using two kinds of achiral thiols to interact with various chiral small aromatic molecules: one thiol improved the affinity between Au NRs and target molecules to produce strong SERS signals of the analytes; meanwhile, the SERS signals of the other thiol were enantioselectively changed to indicate the chirality of the analytes. Using this ingenious strategy, molecule-specific identification and chiral discrimination were simultaneously achieved in SERS spectra.

Herein, we aimed to propose an elegant Raman spectroscopic method to differentiate between amino acids enantiomers based on their selective interactions with suitable chiral selectors. In this work, a simple chiral selector, *i.e.*, gold nanoparticles (NPs) modified with cysteine (Cys) amino acids, were one-step synthesized and then enantioselectively interplayed with tyrosine (Tyr) or phenylalanine (Phe). Differences in Raman scattering signals between D- and L-Tyr (or Phe) were easily detected, which is useful for enantioselective recognition and determination of enantiomeric excess. This work also demonstrated the promising potentials of Raman spectroscopy in revealing the chiral interactions among biomolecules.

Experimental

Synthesis of cysteine (Cys)-modified gold (Au) nanoparticles ("D-Cys-Au" and "L-Cys-Au")

15 mL of a $HAuCl_4$ solution (0.02 mol L^{-1}) was mixed with 15 mL of a trisodium citrate dihydrate solution (0.02 mol L^{-1}). Then, 0.3 mL of ice-cooled $NaBH_4$ solution (0.10 mol L^{-1}) was slowly dropped into the above mixture with stirring, followed by the addition of a D-Cys solution (5 mL, 0.03 mol L^{-1}). After stirring for 2 h in the dark at room temperature, D-Cys-modified Au NPs (defined as "D-Cys-Au") were obtained. By replacing D-Cys with L-Cys, L-Cys-modified Au NPs ("L-Cys-Au") were synthesized using the same procedure as above.

Characterizations

Transmission electron microscopy (TEM) images were recorded on a JEM-2100F instrument equipped with an energy dispersive spectrometer (EDS). Electronic circular dichroism (CD) and UV-vis absorption spectra were simultaneously obtained on a JASCO-1500 spectropolarimeter. A Jobin Yvon confocal laser Raman system (SuperLabRam II) was used to record the Raman spectra. The Raman spectra were collected using a 633 nm laser of after an exposure time of 8 s and three accumulations.

Results and discussion

According to the TEM images, both "D-Cys-Au" (Fig. 1a) and "L-Cys-Au" (Fig. 1b) are NPs in appearance, with an average size of around 5 nm, with the EDS mapping confirming that the NPs are gold NPs (data not shown). As shown in Fig. 1c, the UV-vis absorption spectrum of "D-Cys-Au" is similar to that of "L-Cys-Au": the absorption bands below 300 nm are assigned to D-Cys (or L-Cys) and the bands at around 530 nm to the SPR modes of the Au NPs, which confirm the co-existence of Cys and Au. In the CD spectra of "L-Cys-Au" (Fig. 1d), a broad positive CD signal with a peak at around 203 nm is observed in the range between 200 and 250 nm, which is the mirror image of the negative CD signal of "D-Cys-Au". This pair of CD signals can be attributed to D-Cys and L-Cys. However, CD signals were not detected corresponding to the SPR bands of the Au NPs at around 530 nm, indicating that the as-synthesized Au NPs are not chiroptically active in spite of the addition of chiral D-Cys (or L-Cys) molecules.

In proteins, hydrogen bonds are widespread among amino acid residues to maintain their helical structures. Hence, the modification of Au NPs using D-Cys (or L-Cys) provides the possibility of chiral interactions with other amino acids. We firstly used D-tyrosine (D-Tyr) and L-tyrosine (L-Tyr) as models to check the enantioselective recognition performance of "D-Cys-Au" using CD spectroscopy. Three types of Tyr solutions with the same concentration (1.00×10^{-5} mol L^{-1}) were employed, including: (1) pure D-Tyr; (2) pure L-Tyr; and (3) containing both D-Tyr and L-Tyr (the mol ratio between D-Tyr

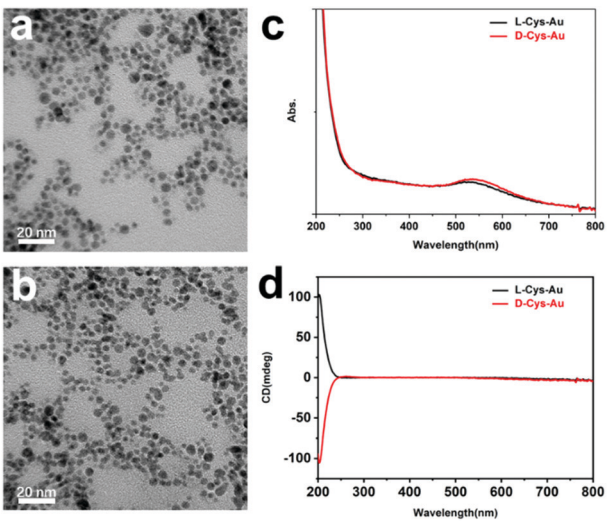

Fig. 1 TEM images of (a) "D-Cys-Au" and (b) "L-Cys-Au"; (c) UV-vis absorption and (d) CD spectra of "D-Cys-Au" (red lines) and "L-Cys-Au" (black lines).

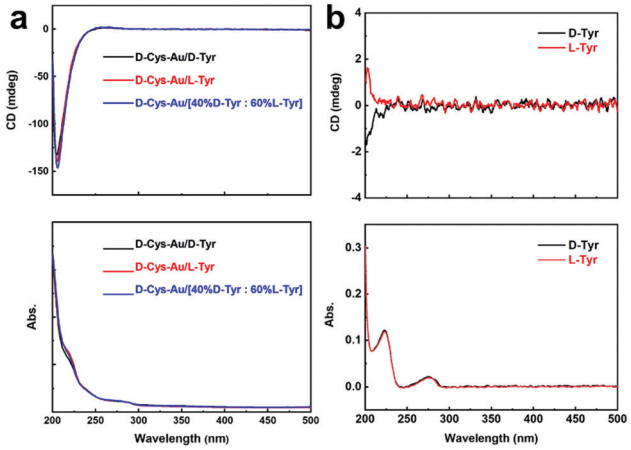

Fig. 2 CD (top) and UV-vis absorption (bottom) spectra of (a) "D-Cys-Au/D-Tyr" (black lines), "D-Cys-Au/L-Tyr" (red lines) and "D-Cys-Au/[40%D-Tyr : 60%L-Tyr]" (blue lines); (b) D-Tyr (black lines) and L-Tyr (red lines).

and L-Tyr is 40 : 60), which is denoted by [40%D-Tyr : 60%L-Tyr]. After mixing "D-Cys-Au" solution with the given Tyr solution above, the CD and UV-vis absorption spectra of the as-prepared mixture were simultaneously recorded. For these three types of mixtures (*i.e.*, "D-Cys-Au/D-Tyr", "D-Cys-Au/L-Tyr", and "D-Cys-Au/[40%D-Tyr : 60%L-Tyr]"), their CD spectra with negative peaks at around 205 nm seem to be quite similar (Fig. 2a), and resemble the CD spectrum of "D-Cys-Au" (Fig. 1d). Also, their UV-vis absorption spectra are almost identical (Fig. 2a, bottom) with two additional peaks at around 219 and 280 nm, which are not observed in the absorption spectrum of "D-Cys-Au" (Fig. 1c). For comparison, the CD and UV-vis absorption spectra of the pure D-Tyr and pure L-Tyr solutions are shown in Fig. 2b. D-Tyr and L-Tyr exhibited nearly the same UV-vis absorption spectra, with two absorption bands at *ca.* 223 and 275 nm. However, they possess opposite CD signals between 200 and 230 nm (Fig. 2b, top), and the wavelength range of these CD signals overlaps with that of "D-Cys-Au". Unfortunately, the CD signals of Tyr are undiscernible after the mixing of "D-Cys-Au", which should be overwhelmed by the strong CD signals of "D-Cys-Au". Therefore, the presence of Tyr could be verified in the UV-vis absorption spectra but not the CD spectra. However, the use of both CD and UV-vis absorption spectroscopy is not straightforward in revealing the chirality of Tyr added into a "D-Cys-Au" solution.

It is known that Raman scattering signals are sensitive to intermolecular interactions, and therefore we tried to check whether enantiomer-dependent differences would be observed in the Raman spectra. For this purpose, a solution of "D-Cys-Au" (or "L-Cys-Au") was first spread and dried on an Al foil-coated slide and then subjected to Raman spectroscopy. The Raman spectrum of "D-Cys-Au" is almost the same as that of "L-Cys-Au" (Fig. 3a), indicating that normal Raman spectroscopy cannot distinguish between D-Cys and L-Cys. In the Raman spectra, several signals at around 499, 680 and 780 cm^{-1} are observed; however, these Raman bands are consistent with those of cystine,[19] which is the dimer of cysteine obtained *via* the

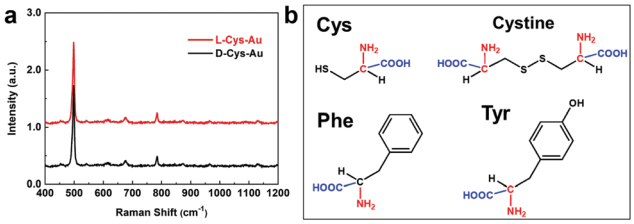

Fig. 3 (a) Raman spectra of "D-Cys-Au" (black line) and "L-Cys-Au" (red line); (b) molecular structures of Cys, cystine, Tyr and Phe.

formation of an S–S bond by two –SH groups of cysteine (see the molecular structures in Fig. 3b). Because the D-Au-Cys solution was dried in air prior to the Raman measurements, the oxidation of cysteine into cystine occurred and the signal at around 499 cm^{-1} is characteristic of the S–S bonding in cystine.

To check the ability of "D-Cys-Au" to discriminate between the Tyr enantiomers, six types of Tyr solutions were prepared with different mol ratios of D-Tyr and L-Tyr, and the total concentration of D-Tyr and L-Tyr was kept as 1.00×10^{-5} mol L^{-1}. These solutions are denoted as [*X*%D-Tyr : (100 − *X*)%L-Tyr], where the mol ratio of D-Tyr and L-Tyr is denoted as *X*% and (100 − *X*)% (*X* = 0, 20, 40, 60, 80, 100). 10 μL of "D-Cys-Au" solution was first mixed with 10 μL of a given [*X*%D-Tyr : (100 − *X*)%L-Tyr] solution for ten minutes, and then the mixture was dropped onto a Al foil-coated slide, dried in air and subjected to Raman spectroscopy. In the Raman spectra of these six types of "D-Cys-Au/[*X*%D-Tyr : (100−*X*)%L-Tyr]" mixtures, together with the characteristic signals of cystine (Fig. 4a), new Raman signals at around 830 and 844 cm^{-1} appear (Fig. 4a), which can be attributed to a Tyr doublet.[20] For pure L-Tyr (*X*% = 0%), its Raman signal intensity at 830 cm^{-1} (denoted by I_{830}) is quite weak. However, I_{830} increased gradually with the mol ratio of D-Tyr (*X*%) and reached a maximum for pure D-Tyr (*X*% = 100%), which is around four times higher than that of pure L-Tyr. Furthermore, the relationship between I_{830} and *X*% can be fitted

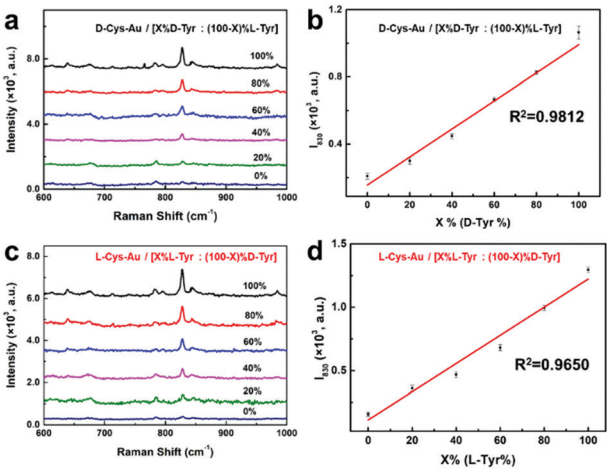

Fig. 4 (a) Raman spectra of the "D-Cys-Au/[*X*%D-Tyr : (100 − *X*)%L-Tyr]" mixture; (b) the linear relationship between I_{830} and the mol ratio of D-Tyr (*X*%); (c) Raman spectra of the "L-Cys-Au/[*X*%L-Tyr : (100 − *X*)%D-Tyr]" mixture; (d) linear regression between I_{830} and the mol ratio of L-Tyr (X%).

as a linear increasing progression plot, with a goodness-of-fit (R^2) value of 0.9811 (Fig. 4b).

Similarly, the discrimination ability of "L-Cys-Au" was also probed using six types of solutions [X% L-Tyr : (100 − X)%D-Tyr], where the mol ratio of L-Tyr and D-Tyr is X% and (100 − X)% (X = 0, 20, 40, 60, 80, 100). Again, in the Raman spectra of these six types of "L-Cys-Au/[X%L-Tyr : (100 − X)%D-Tyr]" mixtures, the signals of Tyr are observed at 830 and 844 cm^{-1} (Fig. 4c). Different from "D-Cys-Au", the I_{830} of pure L-Tyr is the highest, which is around 8-fold higher than that of pure D-Tyr. Also, I_{830} increases linearly with the mol ratio of L-Tyr (X%) (Fig. 4d). Consequently, a kind of chirality preference can be described as follows: "D-Cys-Au" enhances the Raman scattering intensities of D-Tyr, whereas "L-Cys-Au" boosts L-Tyr. Moreover, the above linear relationships between I_{830} and the mol ratio of D-Tyr (or L-Tyr) are useful in differentiating the chirality of Tyr enantiomers and to assess e.e.

Since the molecular structures of phenylalanine (Phe) are similar to those of Tyr (see Fig. 3b), we also checked whether D-Phe and L-Phe could be discriminated between using "D-Cys-Au" as the selector. Six types of Phe solutions were tested with variable ratios of D-Phe to L-Phe, which are defined as [X%D-Phe : (100 − X)%L-Phe] (X% is the mol ratio of D-Phe, X = 0, 20, 40, 60, 80, 100). In the Raman spectra of "D-Cys-Au/[X%D-Phe : (100 − X)%L-Phe]", the emerging Raman bands at around 1004 cm^{-1} (the deformation of the benzene ring) are characteristic of Phe (Fig. 5a).[21] And, the signal intensity at 1004 cm^{-1} (I_{1004}) also grows linearly with the mol ratio of D-Phe (X%) (Fig. 5b), implying the differentiation between D-Phe and L-Phe on cysteine-modified Au NPs.

To understand the roles played by the Au NPs and Cys in the enantiomeric discrimination in the Raman spectra above, two control experiments were conducted. Firstly, Au NPs were prepared without the addition of cysteine and then mixed with D-Tyr (or L-Tyr) to prepare a "Au/D-Tyr" (or "Au/L-Tyr") mixture. As shown in Fig. 6a, the Raman spectrum of "Au/D-Cys" shows only slight differences from that of "Au/L-Cys". Secondly, by directly mixing L-Cys with D-Tyr (or L-Tyr), the as-collected Raman spectrum of "L-Cys/D-Tyr" also resembles that of "L-Cys/L-Tyr" (Fig. 6b).

Based on the two control experiments above (Fig. 6), it seems that both Cys and the Au NPs are essential in the chiral differentiation of Tyr (or Phe). As shown in the CD spectra in Fig. 1d, the as-prepared Au NPs do not exhibit chiroptical

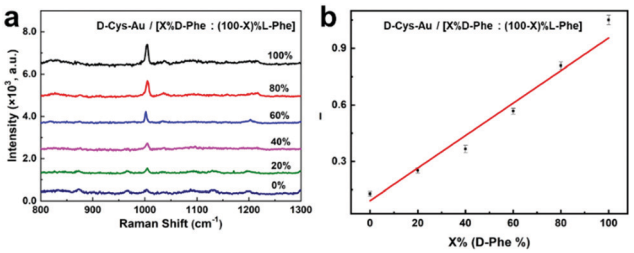

Fig. 5 (a) Raman spectra of the "D-Cys-Au/[X%D-Phe : (100 − X)%L-Phe]" mixture; (b) the linear relationship between I_{1004} and the mol ratio of D-Tyr (X%).

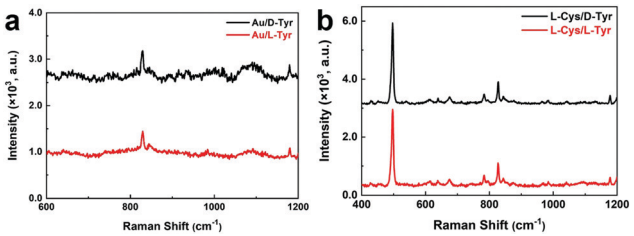

Fig. 6 Raman spectra of (a) "Au/D-Tyr" (black line) and "Au/L-Tyr" (red line); (b) "L-Cys/L-Tyr" (red line) and "L-Cys/D-Tyr" (black line).

activity, even in the presence of chiral Cys, implying the lack of a chiral structure of the Au NPs. Consequently, the possibility of the occurrence of chiral interactions between naked Au NPs and Tyr should be very low. In contrast, chiral intermolecular interactions are feasible between Cys and Tyr because both of them possess chiral carbon atoms. However, without Au NPs, the Raman enantiomeric differentiation of Tyr using free Cys was not achieved. Therefore, this suggests that the enantioselective recognition is a result of the synergetic effects between the Au NPs and Cys, in terms of the following points:

(1) On the chiral carbon atoms of amino acids, the amino ($-NH_2$) and carboxyl (–COOH) groups are connected, which can form hydrogen bonds with other amino acids. The numbers and positions of hydrogen bonds among these groups are controlled by the configurations of the amino acids, which play a key role in chiral recognition. However, there is a thiol group (–SH) on Cys, which can form hydrogen bonds with amino and carboxyl groups, and may thus affect the hydrogen bonding on chiral carbon atoms and thus disturb enantioselective recognition. Due to the high affinity between the thiol group and Au atoms, the disturbance of the thiol would be greatly weakened after the absorption of Cys onto the Au NPs. To some extent, it is reasonable that "D-Cys-Au" (or "L-Cys-Au") show better enantiomeric differentiation performance than free D-Cys (or L-Cys).

(2) When the handedness tags of Cys and Tyr are the same (denoted by DD or LL, *e.g.*, "D-Cys-Au/D-Tyr"), the Raman signal intensities of Tyr are higher than those with opposite tags (denoted by DL or LD, *e.g.*, "D-Cys-Au/L-Tyr"). According to the three-point interaction model for chiral recognition, there are three interaction sites between a D-selector and D-enantiomer. By contrast, there are fewer than three sites between the D-selector and L-enantiomer.[22] In previous research, it has been reported that there are more hydrogen bonds among amino acids with the same handedness tags (DD or LL) than those with the opposite tags (DL or LD).[23]

(3) Because of the SERS effect of the Au NPs, the Raman scattering of D-Tyr near to Au surfaces would be enhanced. The possible steric effect of the benzyl ring on Tyr is disadvantageous to the absorption of Tyr onto the surfaces of Au NPs with Cys modification. In the case of "D-Cys-Au", as discussed above, "D-Cys-Au" interacts with D-Tyr more strongly than L-Tyr due to them having the same handedness tags. In this way, the local concentration of D-Tyr (Scheme 1a) close to the surfaces of the Au NPs should be higher than L-Tyr (Scheme 1b), thus the

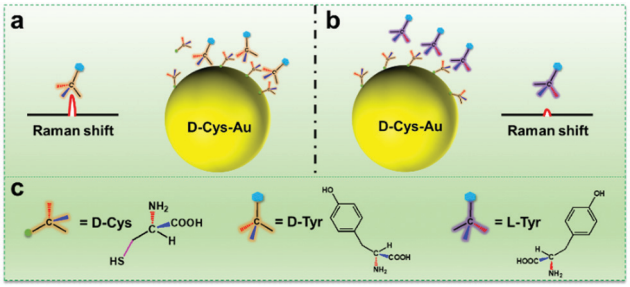

Scheme 1 Proposed mechanism for enantiomeric differentiation using Raman spectra.

Raman signals from D-Tyr are increased. In the case of "L-Cys-Au", the intensity of L-Tyr is higher. Because of the high similarity of the molecular structures of Tyr and Phe, the chiral recognition mechanism of Tyr could be applied to Phe.

(4) It should be noted that the Raman signals intensities of the molecules on the Au NPs are influenced by many other factors (*e.g.*, orientation) except for local concentration,[24] with the proposed mechanism (Scheme 1) still speculative and needing to be verified by more calculations and experimental evidence.

Conclusions

In summary, we propose a Raman spectroscopy method to reveal the enantioselective interactions between Cys and Tyr (or Phe) amino acids on Au NPs, which is sensitively reflected by the characteristic Raman scattering intensity changes of Tyr (or Phe). On the whole, Cys and Tyr (or Phe) enantiomers with same chirality result in the stronger Raman scattering of Tyr (or Phe) of over several folds than those with opposite chirality. Thanks to the Raman signals intensity difference detailed above, enantioselective recognition and determination of enantiomeric excess is feasible. Interestingly, the common chiral analysis method of CD spectroscopy cannot detect such chiral interactions, which implies the advantages (*e.g.*, high sensitivity and specificity) and potential of using Raman spectroscopy in chiral analysis by virtue of molecular vibrational information.

Author contributions

Xueping Sun: conceptualization, investigation, data curation, writing – original draft. Ning Wang: investigation, data curation, writing – original draft. Yanxiu He: investigation, visualization. Huanjun Kong: investigation, visualization. Haifeng Yang: funding acquisition, writing – review and editing; Xinling Liu: funding acquisition, supervision, project administration, writing – review and editing.

Conflicts of interest

There are no conflicts to declare.

Acknowledgements

This work is supported in part by the National Natural Science Foundation of China (No. 21475088), the International Joint Laboratory on Resource Chemistry (IJLRC) and the Shanghai Key Laboratory of Rare Earth Functional Materials.

Notes and references

1 B. Kasprzyk-Hordern, *Chem. Soc. Rev.*, 2010, **39**, 4466–4503.
2 E. G. Shcherbakova, T. D. James and P. Anzenbacher, *Nat. Protoc.*, 2020, **15**, 2203–2229.
3 J. E. Hein and D. G. Blackmond, *Acc. Chem. Res.*, 2012, **45**, 2045–2054.
4 J. J. A. J. Bastings, H. M. van Eijk, S. W. Olde Damink and S. S. Rensen, *Nutrients*, 2019, **11**, 2205.
5 Y. Ma, L. Shi, H. Yue and X. Gao, *Colloids Surf., B*, 2020, **195**, 111268.
6 P. Zhou, J. Q. Wang, M. Wang, J. Hou, J. R. Lu and H. Xu, *J. Colloid Interface Sci.*, 2019, **548**, 244–254.
7 N. Gao, Z. Du, Y. Guan, K. Dong, J. Ren and X. Qu, *J. Am. Chem. Soc.*, 2019, **141**, 6915–6921.
8 W. Jiang, M. S. Pacella, H. Vali, J. J. Gray and M. D. McKee, *Sci. Adv.*, 2018, **4**, eaas9819.
9 A. Bigdeli, F. Ghasemi, N. Fahimi-Kashani, S. Abbasi-Moayed, A. Orouji, Z. J. N. Ivrigh, F. Shahdost-Fard and M. R. Hormozi-Nezhad, *Analyst*, 2020, **145**, 6416–6434.
10 J. C. Sutherland, *Compr. Chiropt. Spectrosc.*, 2011, **ch2**, 35–63.
11 Z. Chen, Q. Wang, X. Wu, Z. Li and Y.-B. Jiang, *Chem. Soc. Rev.*, 2015, **44**, 4249–4263.
12 I. Pérez-Jiménez, D. Lyu, Z. Lu, G. Liu and B. Ren, *Chem. Sci.*, 2020, **11**, 4563–4577.
13 T. J. Wenzel and C. D. Chisholm, *Chirality*, 2011, **23**, 190–214.
14 H.-E. Lee, H.-Y. Ahn, J. Mun, Y. Y. Lee, M. Kim, N. H. Cho, K. Chang, W. S. Kim, J. Rho and K. T. Nam, *Nature*, 2018, **556**, 360–365.
15 N. V. Karimova and C. M. Aikens, *Part. Part. Syst. Charact.*, 2019, **36**, 21.
16 Y. Kalachyova, O. Guselnikova, R. Elashnikov, I. Panov, J. Zadny, V. Cirkva, J. Storch, J. Sykora, K. Zaruba, V. Svorcik and O. Lyutakov, *ACS Appl. Mater. Interfaces*, 2019, **11**, 1555–1562.
17 O. Guselnikova, P. Postnikov, A. Trelin, V. Svorcik and O. Lyutakov, *ACS Sens.*, 2019, **4**, 1032–1039.
18 Y. Wang, X. Zhao, Z. Yu, Z. Xu, B. Zhao and Y. Ozaki, *Angew. Chem., Int. Ed.*, 2020, **59**, 19079–19086.
19 X. Sun, H. Kong, Q. Zhou, S. Tsunega, X. Liu, H. Yang and R.-H. Jin, *Anal. Chem.*, 2020, **92**, 8015–8020.
20 L. I. Grace, R. Cohen, T. M. Dunn, D. M. Lubman and M. S. de Vries, *J. Mol. Spectrosc.*, 2002, **215**, 204–219.
21 G. Zhu, X. Zhu, Q. Fan and X. Wan, *Spectrochim. Acta, Part A*, 2011, **78**, 1187–1195.
22 Y. Jeong, H. W. Kim, J. Ku and J. Seo, *Sci. Rep.*, 2020, **10**, 16166.
23 Y. Zhou, H. Sun, H. Xu, S. Matysiak, J. Ren and X. Qu, *Angew. Chem., Int. Ed.*, 2018, **57**, 16791–16795.
24 M. Moskovits and J. S. Suh, *J. Phys. Chem.*, 1984, **88**, 5526–5530.